ETH zürich

Training of a Classifier for Structural Component Failure based on Hybrid Simulation and Kriging

G. Abbiati, S. Marelli, C. Ligeikis, R. Christenson, B. Stojadinovic

Chair of Risk, Safety and Uncertainty Quantification
Stefano-Franscini-Platz 5
CH-8093 Zürich

Risk, Safety & Uncertainty Quantification

Data Sheet

Journal:	-
Report Ref.:	RSUQ-2020-012
Arxiv Ref.:	https://engrxiv.org/b9kxa/
DOI:	-
Date submitted:	20/11/2020
Date accepted:	-

Training of a Classifier for Structural Component Failure based on Hybrid Simulation and Kriging

G. Abbiati*[1], S. Marelli[2], C. Ligeikis[3], R. Christenson[4], and B. Stojadinovic[2]

[1]*Department of Civil and Architectural Engineering, Aarhus University, Denmark*
[2]*Department of Civil, Environmental and Geomatic Engineering, ETH Zurich, Switzerland*
[3]*Department of Civil and Environmental Engineering, University of Michigan, U.S.*
[4]*Department of Civil and Environmental Engineering, University of Connecticut, U.S.*

Draft submitted to *engrXiv*

January 27, 2021

Abstract

Hybrid simulation is a tool for discovering the inner workings of a tested substructure beyond the linear regime. Hybrid simulation is conducted to reproduce the response of a prototype in scaled or real time using a hybrid model that combines physical and numerical substructures interacting with each other in a feedback loop. As a result, the tested substructure interacts with a realistic assembly subjected to a credible loading scenario. The obtained low-quantity-high-value experimental data is used to conceive and calibrate computational models for nonlinear structural analysis in the current practice. Instead, this paper extends the scope of hybrid simulation to constructing a safe/failure state classifier for the tested substructure by adaptively designing a sequence of parametrized hybrid simulations. Such a classifier is intended to compute the state of any physical-substructure-like component within system-level numerical simulations. The proposed procedure is experimentally validated for a three-degrees-of-freedom hybrid model subjected to Euler buckling.

Keywords: Hybrid simulation; meta-modeling; Kriging; active learning; classifier; buckling.

1 Introduction

Hybrid Simulation (HS) is a dynamic simulation paradigm that merges physical experiments and computational models. In mechanical and electrical engineering, such an approach is known as hardware-in-the-loop simulation. The report by Schellenberg and co-authors (Schellenberg et al., 2009) provides a comprehensive overview of state-of-art HS methods and algorithms. In detail, HS is conducted using a hybrid model, which combines physical and numerical substructures (NS and PS, respectively) that interact with each other in a real-time feedback loop, to simulate the time history response of a prototype structure subjected to a realistic excitation. The PS is tested in the laboratory using servo-controlled actuators equipped with force and displacement transducers. The NS replaces those substructures that can be reliably simulated (e.g., masses or components whose response remains in the linear regime) or would exceed the testing capacities of the experimental facility. A time integration algorithm coordinates the HS ensuring interface

*Corresponding Author: Dr. Giuseppe Abbiati, abbiati@eng.au.dk, ORCID: 0000-0002-5048-8505.

force balance and displacement compatibility between NS and PS. As a result, HS reproduces the time history response of the prototype structure subjected to a realistic excitation. When the PS response is rate-independent, it is good practice to perform HS with an extended time scale from 50-200 times slower than real-time in order to improve control accuracy. Time scaling enables full-scale experimentation without the need for large oil-flow demand. In earthquake engineering, HS is used for testing large structures such as bridges (e.g., (Mosqueda et al., 2008; Abbiati et al., 2015)) and buildings (e.g., (Yang et al., 2009; Bursi et al., 2012)). Similarly, testing of floating structures with a sizeable scaling factor in hydrodynamic laboratories is challenging due to the extent of mooring line footprints, which can range from two to four times the water depth. For this reason, HS has been recently proposed to truncate mooring lines whose missing parts are simulated as NS (e.g., (Sauder et al., 2018; Vilsen et al., 2019)). Hybrid fire testing originated in response to limitations of standard fire tests to account for a realistic internal force redistribution caused by thermal expansion or partial collapse of tested assemblies. (e.g., (Whyte et al., 2016; Abbiati et al., 2020)).

Regardless of the specific domain of application, HS is a tool for discovering the inner workings of a structural system in the nonlinear regime with few significant experiments. The information carried by low-quantity-high-value experimental data produced via HS is used to conceive and calibrate computational models for structural analysis (Bursi et al., 2017). In this context, the set of loading scenarios explored via HS corresponds to the domain of validity of developed computational models. The usability of those computational models outside such domain is tightly related to the generalization error concept, which indicates the prediction errors for unobserved combinations of loading histories and boundary conditions (Roy and Oberkampf, 2011; Worden et al., 2020). The damage pattern characterizing civil engineering structures typically involves debonding of heterogeneous materials (e.g., concrete and steel), crack opening (e.g., steel beam-column connections, concrete members or masonry elements), buckling and yielding (e.g., steel rebars or members). To reproduce such damage features, highly nonlinear expensive-to-evaluate computational models are necessary. The computational cost of such models is seldom affordable beyond the scale of a single structural component (e.g., beam-to-column joint). Also, usually, little physical justification supports some of the parameters, which are tuned to match available experimental observations.

Instead of supporting the development of a computational model of the PS, this paper proposes to expand the scope of HS to training a classifier to determine the *failed* or *non-failed* state of the PS. The parameter space defining loading and boundary conditions of the hybrid model is the support of the classifier, which can be reasonably assumed as the domain of validity for numerical predictions. To greedily construct a safe/failure domain classifier at the lowest experimental cost possible, an initial random sampling of the parameter space is adaptively enriched using kriging meta-models (Santner et al., 2003) and active learning (Vapnik, 2013).

The proposed method, namely active-learning-kriging hybrid-simulation (AK-HS), relies on an adaptation of the active-learning kriging Monte Carlo simulation algorithm from the field of structural reliability (Echard et al., 2011). The idea of combining the active-learning kriging Monte Carlo simulation algorithm and HS was originally proposed in (Abbiati et al., 2017) and applied in (Ligeikis and Christenson, 2020) to compute the probability of failure of a hybrid model with uncertain parameters. However, the computed failure probability has no utility outside the context of the examined prototype structure. Besides providing a comprehensive experimental validation of the AK-HS method, the main contribution of this paper lies in the direct link established between structural testing, performed using HS, and the computation of a safe/failure state classifier for the PS. Such a classifier is intended to determine the state of any component of the same type of the tested PS within a system-level, rather than a component-level, numerical simulation. In doing that, one must verify that, for every PS-like component, boundary conditions and loading must stay within the range explored via HS.

The effectiveness of the AK-HS method is illustrated for a 3-degrees-of-freedom (3-DoFs) prototype structure, which consists on an elastically restrained beam subjected to constant axial loading. Failure is associated with Euler buckling, which may occur or not depending on the rotational stiffness of the restraints. Experimental results are validated against the analytical model proposed by Newmark (Bažant and Cedolin, 2010).

The paper is organized as follows. Section 2 describes the AK-HS method. Section 3 describes the experimental validation of the method, the results of which are discussed in Section 4. Finally, conclusions and future outlook are given in Section 5.

2 Introducing active learning into hybrid simulation

Let us denote with $\mathbf{X} = \{X_1, \ldots, X_M\}$ an M-dimensional vector of input variables to parametrize the NS, the PS and the loading excitation (or a subset of these) of the hybrid model of the prototype structure, and with Y a generic response Quantity of Interest (QoI) of the hybrid model. A mapping $\mathcal{M}$ between input variables and a single QoI reads,

$$\mathbf{X} \in \mathcal{D}_{\mathbf{X}} \subset \mathbb{R}^M \mapsto Y = \mathcal{M}(\mathbf{X}) \subset \mathbb{R} \tag{1}$$

It can be argued that the inherent variability of the hybrid model response obtained with nominally identical PSs, as well as measurement noise, requires a stochastic mapping between input variables and QoIs. However, the scope of this paper is limited to the case of PS with almost deterministic behavior. Moreover, relevant studies testify that measurement noise of standard structural testing equipment has a negligible effect on the prototype structure response evaluated via HS with modern hardware (Ahmadizadeh and Mosqueda, 2009; Abbiati et al., 2018). Therefore, $\mathcal{M}$ is assumed to be deterministic.

The failure domain $\mathcal{D}_f \in \mathcal{D}_{\mathbf{X}}$ is defined as the region of the input parameter space where the hybrid model response QoI is greater or equal than a given threshold value y_{adm},

$$\mathbf{x} \in \mathcal{D}_f : \mathcal{M}(\mathbf{x}) \geq y_{adm} \tag{2}$$

Computing $\mathcal{D}_f$ means solving a classification problem where every sample $\mathbf{x}$ is categorized either as failed or non-failed. However, since it entails testing of the PS, $\mathcal{M}(\mathbf{x})$ can be assimilated to an expensive-to-evaluate *black-box* model. In order to make such a classification problem tractable, kriging meta-modeling is introduced to surrogate the hybrid model response,

$$Y \approx \hat{Y} = \hat{\mathcal{M}}(\mathbf{X}) \tag{3}$$

The kriging meta-model adaptively drives the choice of the next sample $\mathbf{x}$ to evaluate via HS so that the convergence of the limit state surface, which separates failure and non-failure domains, requires a minimal number of experiments. The choice of samples to be evaluated can be considered as a dilemma between the exploration and the exploitation of the input parameter space. Active learning (Settles, 2009) addresses this problem by providing algorithms for selecting the most informative sample against the solution of a specific supervised learning problem, which, in this case, corresponds to the identification of the boundaries of the failure domain. After recalling the basics of kriging surrogate modeling, the AK-HS procedure is outlined.

2.1 Basics of kriging meta-modeling

Kriging is a surrogate modeling technique that considers the computational model to be a realization of a Gaussian process,

$$\hat{\mathcal{M}}(\mathbf{x}) = \boldsymbol{\beta}^T \mathbf{f}(\mathbf{x}) + \sigma^2 Z(\mathbf{x}, \omega) \tag{4}$$

where $\mathbf{f}(\mathbf{x}) = [f_1(\mathbf{x}), \ldots, f_p(\mathbf{x})]$ are regression functions, $\boldsymbol{\beta}$ is a vector of coefficients, which compose the mean value of a Gaussian process. σ^2 is the corresponding variance. $Z(\mathbf{x}, \omega)$ is a zero-mean, unit-variance, stationary Gaussian process, which is characterized by an autocorrelation function $R(|\mathbf{x} - \mathbf{x}'|; \boldsymbol{\rho})$ and its hyper-parameters ρ. The kriging model is trained with a set of realizations $\boldsymbol{\mathcal{X}} = \{\boldsymbol{\mathcal{X}}^{(i)}, i = 1, \ldots, N\}$ and the corresponding responses of the computational model $\boldsymbol{\mathcal{Y}} = \{\mathcal{M}\left(\boldsymbol{\mathcal{X}}^{(i)}\right), i = 1, \ldots, N\}$, which together form the so-called Experimental Design (ED) $\{\boldsymbol{\mathcal{X}}, \boldsymbol{\mathcal{Y}}\}$. Kriging parameters are obtained by generalized least-squares solution:

$$\boldsymbol{\beta}(\boldsymbol{\rho}) = \left(\mathbf{F}^T \mathbf{R}^{-1} \mathbf{F}\right)^{-1} \mathbf{F}^T \mathbf{R}^{-1} \boldsymbol{\mathcal{Y}} \tag{5}$$

$$\sigma_y^2(\boldsymbol{\rho}) = \frac{1}{N} (\boldsymbol{\mathcal{Y}} - \mathbf{F}\boldsymbol{\beta})^T \mathbf{R}^{-1} (\boldsymbol{\mathcal{Y}} - \mathbf{F}\boldsymbol{\beta}) \tag{6}$$

where $\mathbf{R}_{ij} = R\left(|\boldsymbol{\mathcal{X}}^{(i)} - \boldsymbol{\mathcal{X}}^{(j)}|; \boldsymbol{\rho}\right)$ is the correlation matrix and $\mathbf{F}_{il} = f_l\left(\boldsymbol{\mathcal{X}}^{(i)}\right)$. In practice the correlation hyper-parameters are unknown and their values shall be inferred by e.g. maximum likelihood estimation. Having determined the kriging parameters, the prediction value of the computational model at a point $\mathbf{x} \in \mathcal{D}_{\mathbf{X}}$ is a Gaussian variable with the following mean value and variance:

$$\mu_{\hat{Y}}(\mathbf{x}) = \boldsymbol{\beta}^T \mathbf{f}(\mathbf{x}) + \mathbf{r}(\mathbf{x})^T \mathbf{R}^{-1} (\boldsymbol{\mathcal{Y}} - \mathbf{F}\boldsymbol{\beta}) \tag{7}$$

$$\sigma_{\hat{Y}}(\mathbf{x}) = \sigma_y^2 \left(1 - \mathbf{r}(\mathbf{x})^T \mathbf{R}^{-1} \mathbf{r}(\mathbf{x}) + \mathbf{u}(\mathbf{x})^T \left(\mathbf{F}^T \mathbf{R}^{-1} \mathbf{F}\right)^{-1} \mathbf{u}(\mathbf{x})\right) \tag{8}$$

where $\mathbf{r}_i(\mathbf{x}) = R\left(|\mathbf{x} - \boldsymbol{\mathcal{X}}^{(j)}|; \boldsymbol{\rho}\right)$ and $\mathbf{u}(\mathbf{x}) = \mathbf{F}^T \mathbf{R}^{-1} \mathbf{r}(\mathbf{x}) - \mathbf{f}(\mathbf{x})$.

2.2 Adaptive design of hybrid simulations

The purpose of the kriging meta-model is to accurately locate the limit state surface, which separates failed and non-failed states of the PS, regardless the probability measure assigned to the input parameter space. Therefore, all input parameters in $\mathbf{X}$ are assumed to be statistically independent and uniformly distributed. Corresponding ranges must comply with displacement and force capacity of the testing facility.

The kriging meta-model obtained with the procedure stated in Section 2.1, is capable of exactly reproducing the points in the ED set. Indeed, the kriging meta-model is an exact interpolator, meaning that $\mu_{\hat{Y}}\left(\boldsymbol{\mathcal{X}}^{(i)}\right) = \mathcal{M}\left(\boldsymbol{\mathcal{X}}^{(i)}\right), i = 1, \ldots, N$, exactly. This, however, does not mean that such a meta-model accurately reproduces the boundary of the failure domain. Adaptively enriching the ED set in a guided way can improve the accuracy of the trained kriging meta-model in predicting the failure domain of the hybrid model. The proposed learning rule is an adaptation of the adaptive kriging algorithm proposed by Echard et al. (Echard et al., 2011) for failure probability estimation problems and later extended to quantile estimation problems in Schöbi et al. (Schöbi et al., 2017). The main steps of the AK-HS procedure are listed here:

1. Generate an initial ED by sampling $\boldsymbol{\mathcal{X}}$ with a space filling technique (e.g., Sobol' sequence or LHS) and evaluate the corresponding hybrid model response QoIs $\mathcal{Y}^{(i)} = \hat{\mathcal{M}}\left(\boldsymbol{\mathcal{X}}^{(i)}\right)$.

2. Train a kriging meta-model $\hat{\mathcal{M}}$ based on the initial ED $\{\boldsymbol{\mathcal{X}}, \boldsymbol{\mathcal{Y}}\}$ as described in (5) and (5).

3. Generate a large set of samples of the input parameter space $\mathcal{S} = \{\mathbf{x}_1, \ldots, \mathbf{x}_j, \ldots, \mathbf{x}_M\}$ and predict the response values of $\hat{\mathcal{M}}$, i.e., $\mu_{\hat{Y}}(\mathbf{x})$ and $\sigma_{\hat{Y}}(\mathbf{x})$, as described in (7) and (8).

4. Enrich the ED by the taking the sample $\mathbf{x}^* \in \mathcal{S}$ that maximizes the probability of misclassification,

$$\mathbf{x}^* = \underset{\mathbf{x}_j \in \mathcal{S}}{\arg\max} \Phi\left(-\frac{|\mu_{\hat{Y}}(\mathbf{x}_j) - y_{adm}|}{\sigma_{\hat{Y}}(\mathbf{x}_j)}\right) \tag{9}$$

   where $\Phi(\cdot)$ is the cumulative Gaussian distribution function. As can be argued from (9), best candidate samples lie either where the variance of the meta-model is high (exploration) or close to the boundary of the failure domain (exploitation). In both cases, the probability of misclassification tends to its upper bound, which is equal to 0.5.

5. Evaluate the corresponding QoI $y^* = \mathcal{M}(\mathbf{x}^*)$ via HS and add the pair $\{\mathbf{x}^*, \mathbf{y}^*\}$ to the ED.

The procedure loops between Step #2 and Step #5 until a maximum allowed number of experiments N_{max} is reached.

The stopping criterion originally proposed in the paper of Echard et al. (Echard et al., 2011), was defined based on a threshold value for the ratio between confidence interval and average of the failure probability estimate associated with the failure domain $\mathcal{D}_f$. However, as highlighted in the discussion of the results of the validation example (Section 4), the number of experiments necessary to meet such a convergence criterion are not reasonably affordable.

The safe/failure domain classifier is obtained as by-product of the last computed kriging meta-model,

$$\begin{cases} p(Z = F|\mathbf{x}) = 1 - \Phi\left(\frac{\mu_{\hat{Y}}(\mathbf{x}) - y_{adm}}{\sigma_{\hat{Y}}(\mathbf{x})}\right) \\ p(Z = S|\mathbf{x}) = \Phi\left(\frac{\mu_{\hat{Y}}(\mathbf{x}) - y_{adm}}{\sigma_{\hat{Y}}(\mathbf{x})}\right) \end{cases} \tag{10}$$

where F and S indicate *failure* and *safe* states, respectively.

3 Experimental validation of the method

3.1 Prototype structure

In order to validate the proposed procedure, a benchmark experiment was conceived. It consists of a simply-supported beam restrained with linear elastic rotational springs at both ends and subjected to a axial load applied with a linear ramp. This type of structure is common in practice, as most beam-columns are neither truly pinned-pinned nor fixed-fixed. The prototype structure is depicted in Figure 1.

where K_1 and K_2 define the stiffness of left and right rotational restraints. Polar moment of inertia $J_1 = J_2 = 90000$ kgmm^2 and mass $M = 20$ kg provide inertia to the three DoFs of the system, which correspond to rotations of both beam ends and translation of the right end. In

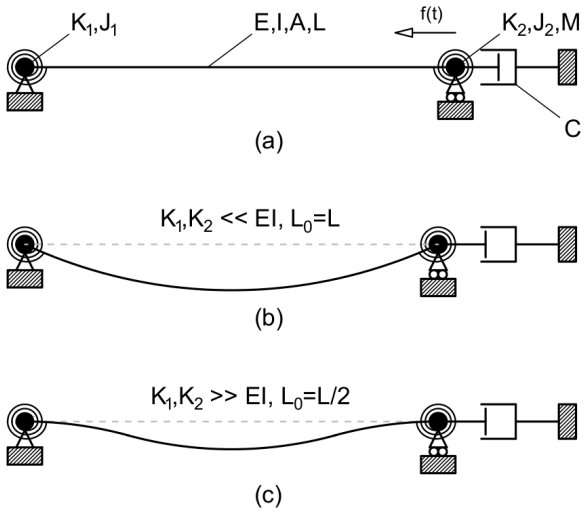

Figure 1: Prototype structure: a) undeformed configuration; b) buckling deformation for the limit case $K_1, K_2 << EI$; c) buckling deformation for the limit case $K_1, K_2 >> EI$.

addition, the horizontal translation of the right support activates a linear dashpot characterized by viscous coefficient $C = 3000$ Ns/mm. The simply-supported beam consists of an aluminum plate with a nominal 200×500 mm footprint and 2 mm thickness. However, the simply-supported length of the beam L was actually shortened to 460 mm, due to the end clamps of the testing rig. Accordingly, the cross-section is characterized by area $A = 400$ mm^2 and a moment of inertia $I = 133.33$ mm^4. An elastic modulus $E = 69500$ MPa a density $\rho = 2700$ kg/m^3 and a Poisson ration $\nu = 0.32$ characterized the material properties of the plate. Furthermore, the effective buckling length of the beam is sensitive to the stiffness of each elastic rotational restraint. In the limit case of $K_1, K_2 << EI$, the effective length L_0 of the beam tends to $L = 460$ mm i.e., pinned-pinned configuration. The opposite case corresponds to $K_1, K_2 >> EI$, the effective length L_0 of the beam tends to $L/2 = 230$ mm i.e., fixed-fixed configuration. The following approximate equation, developed by Newmark, is used to interpolate the buckling load between these two extreme configurations (Bažant and Cedolin, 2010),

$$P_{cr} = \frac{\pi EI}{L^2} \left[\frac{(0.4 + \lambda_1)(0.4 + \lambda_2)}{(0.2 + \lambda_1)(0.2 + \lambda_2)} \right] \tag{11}$$

where $\lambda_1 = \frac{EI}{K_1 L}$ and $\lambda_2 = \frac{EI}{K_2 L}$ account for the relative bending stiffness of the beam compared to the rotational restraints. The lower bound of the buckling load $P_{cr,min} = 432.2$ N corresponds to the pin-pin configuration while the upper bound $P_{cr,max} = 1729$ N to the fixed-fixed configuration. Figure 2 depicts the dynamic substructuring scheme adopted for HS.

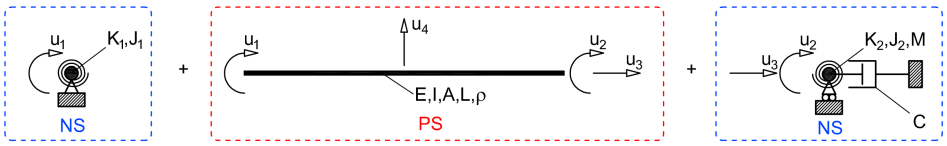

Figure 2: Dynamic substructuring scheme adopted in HS.

With regard to Figure 2, the PS coincides with the 3-DoFs beam, which is tested in the laboratory, while the NS comprises the remaining part of the prototype structure. The rotational and

translational DoFs are denoted by u_1, u_2 and u_3, respectively. The out-of-plane displacement of the beam at its center point, denoted by u_4, is activated by buckling and measured with a laser displacement sensor. It is important to stress that this out-of-plane displacement is not included in the equation of motion of the hybrid model.

3.2 Hybrid simulation setup

The 3-DoFs HS test rig used to conduct the HSs is a stiff loading frame equipped with four electro-mechanical actuators interfaced to an INDEL real-time system (Abbiati et al., 2018). The 3-DoFs HS test rig is designed to test plate specimens with an approximate footprint of 200×500 mm and thickness varying between 1 and 3 mm. Figure 3 illustrates the architecture of the HS setup, including a close-up view of the plate specimen accommodation. The GINLink

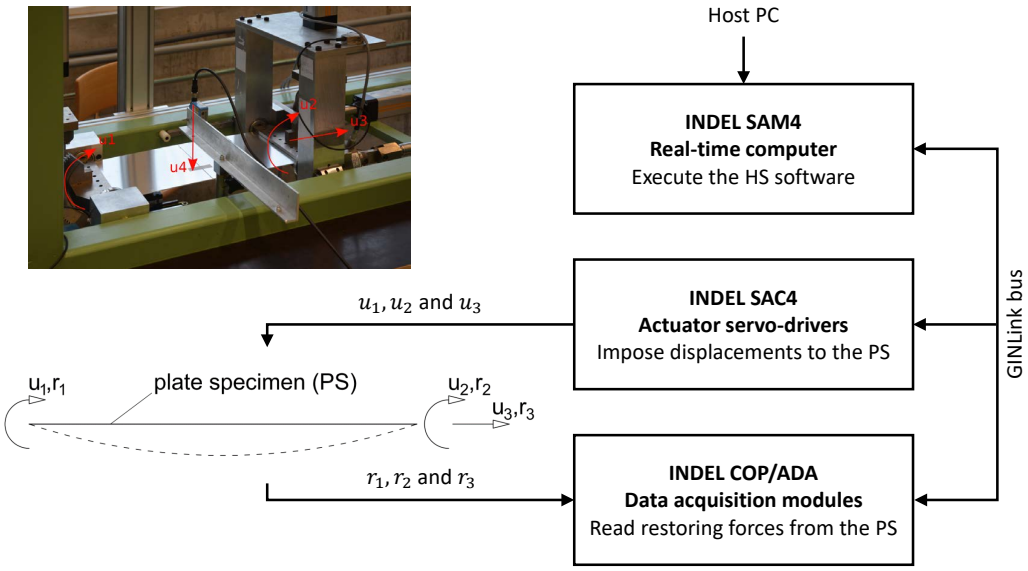

Figure 3: Architecture of the 3-DoFs HS test rig.

bus connects the actuator servo-driver INDEL SAC4 and all data acquisition modules INDEL COP-ADA to the real-time computer INDEL SAM4, which runs the HS software. The latter is developed in the MATLAB/SIMULINK environment and downloaded to the real-time computer INDEL SAM4 via Ethernet from the Host-PC. At each simulation time step, the HS software imposes displacements u_1, u_2 and u_3 to the plate specimen, the PS, reads the corresponding restoring forces r_1, r_2 and r_3 measured using force transducers, and solves the coupled equation of motion of the hybrid model. In addition, a laser sensor measures the out-of-plane deflection at the mid-span of the plate specimen. A detailed description of the time integration scheme adopted to solve the equation of motion is reported in (Abbiati et al., 2019). Figure 4 shows two axonometric views of the 3-DoFs HS test rig, including the main hardware components. In this figure, the gray-colored parts are fixed to the reaction frame, which is not visible, while the moving parts of the 3-DoF HS test rig are colored in yellow. The two rack-pinion systems (10) convert motion along the vertical actuator axes y_1 and y_2 (1) to rotations u_1 and u_2, respectively, which are imposed to the short edges of the plate specimen (6) through aluminum clamps (3). Horizontal actuators along axes x_1 and x_2 (2) control the position of the moving frame (4), which is mounted on two profiled rail guides using ball bearings (5). As a result, the position of the

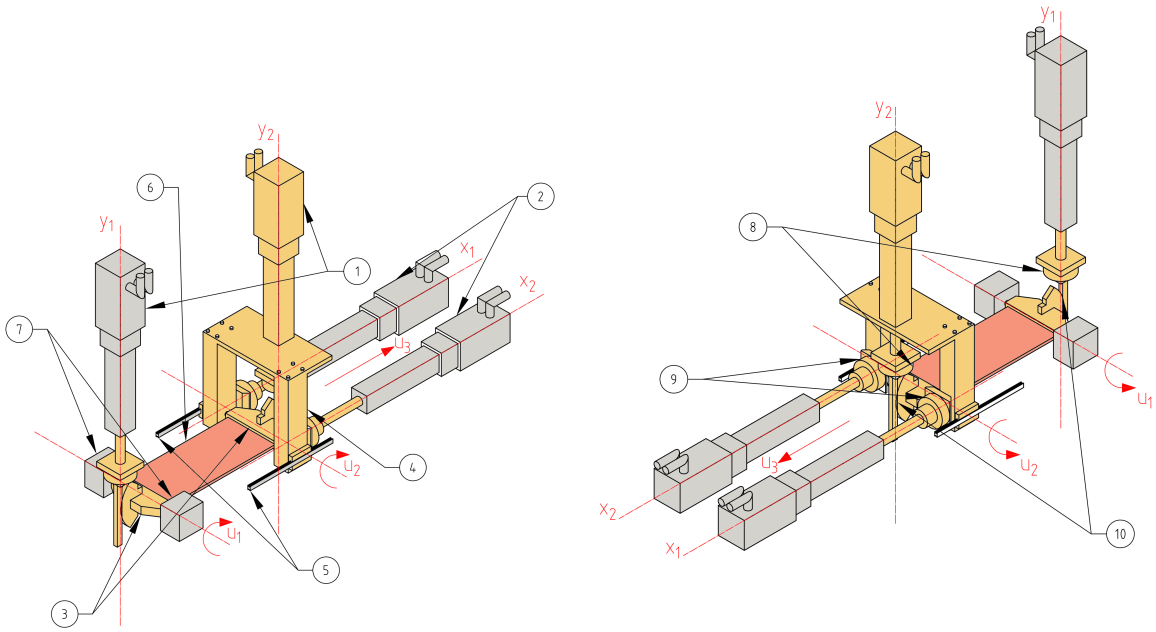

Figure 4: Axonometric views of the 3-DoFs HS test rig with main components: (1) vertical actuators; (2) horizontal actuators; (3) installation clamps; (4) moving frame; (5) profiled rail guides; (6) plate specimen; (7) hinges; (8) vertical actuator load cells; (9) horizontal actuator load cells; (10) rack-pinion systems. The moving parts are colored in yellow while the grey parts are fixed to the reaction frame, which is omitted in this figure for clarity.

moving frame (4) equals the axial elongation of the plate specimen u_3 (6).

The repeatability of the HSs was assessed by comparing the results of three experiments characterized by the same values of rotational stiffness. The force vs. out-of-plane displacement curves for these experiments are shown in Figure 5a. It is clear that the HSs were highly repeatable. In addition, these results confirmed the assumption that the output of the hybrid model is almost deterministic with negligible variability in the PSs. Figure 5b also shows results from three HSs using different rotational stiffness combinations. In general, the experimental data matched well with the theoretical critical buckling loads predicted by (11).

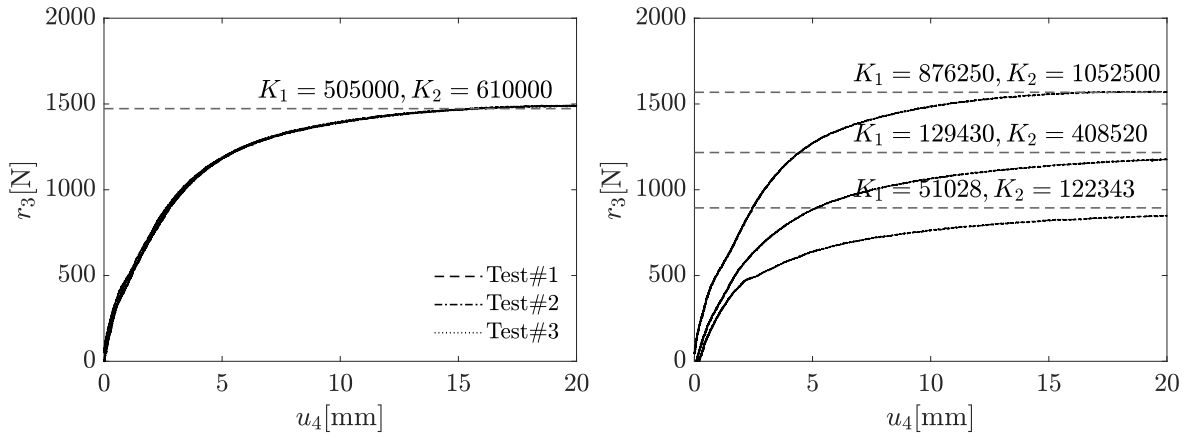

Figure 5: Validation of experimental assumptions: (a) test repeatability and (b) agreement with Newmark's equation predictions (dash lines).

4 Experimental results and discussion

The AK-HS procedure described in Section 2 was applied to train a classifier for the buckling domain of the prototype structure described in Section 3 within the range of the input parameters defined in Table 1. In detail, first, a reference axial load $P_{ref} = 2000$ N was selected to ensure a

Table 1: Input random parameters.

Variable	Distribution	Lower bound	Upper bound	Unit
K_1	Uniform	10000	1000000	$[\frac{Nmm}{rad}]$
K_2	Uniform	20000	1200000	$[\frac{Nmm}{rad}]$

full development of buckling for any pair of $\{K_1, K_2\} \in \mathcal{D}_{\mathbf{X}}$ in the given range. This reference axial load was applied to the hybrid model as a linear increasing ramp of 10 s duration in simulation time. Since hybrid simulations were performed with a testing time scale $\lambda = 50$, each experiment lasted 500 s of wall-clock time. The critical buckling load was taken as the plateau value of the resulting measured force-displacement axial response curve. Such critical load estimated with HS corresponds to the QoI Y, as specified in (3), and accounts for the stiffness of the numerical rotational restraints. It should be noted that all of the experiments conducted were destructive, and thus different (but nominally identical) aluminum plates were used for each hybrid simulation.

The AK-HS procedure described in Section 2 was executed considering a target buckling load of $y_{adm} = 1200$ N. An initial 10-sample ED was generated using a Sobol' sequence and the corresponding buckling loads were estimated using HS. Then, the ED was adaptively enriched with 30 additional samples using the AK-HS procedure. The kriging meta-models were estimated using the UQLab software framework developed by the Chair of Risk, Safety and Uncertainty Quantification at ETH Zurich (Marelli and Sudret, 2014). Figure 6 depicts the meta-models obtained using 10, 20, 30 and 40 samples.

As shown in Figure 6, the classifier trained using the initial ED did not accurately reproduce the buckling domain of the hybrid model. However, after 20 experiments, the failure surface estimated by the classifier already converged toward the analytical solution of provided by Newmark (i.e., using (11)). This result is consistent with the plots of Figure 7, which depicts the convergence of the normalized failure domain area Ω_f and related 95 % confidence interval. The latter corresponds to a failure probability if one assumes a uniform probability measure over $\mathcal{D}_{\mathbf{X}}$. Furthermore, by the end of the experimental campaign, the ED points mostly accumulated along a well-defined failure surface.

Finally, Figure 8 depicts the safe/failure state classifier for two orthogonal sections of the support of the kriging meta-model. It is predicted from the Newmark model of (11) that for a given load of $y_{adm} = 1200$ N, and $K_2 = 600000$ Nmm/rad the system buckles for $K_1 < 98995$ Nmm/rad; and similarly when $K_1 = 500000$ Nmm/rad the system buckles when $K_2 < 107040$ Nmm/rad. As can be appreciated from the plots, the trained classifier fairly agrees with such analytical predictions and it is characterized by a sharp transition between failed and non-failed states.

5 Conclusions

This paper extends the scope of hybrid simulation to training a classifier that determines the *failed* or *non-failed* state of the physical substructure. Kriging meta-models and active learning are used to greedily construct a safe/failure domain classifier at the lowest experimental cost possible. The resulting procedure, namely active-learning-kriging hybrid-simulation, relies on an

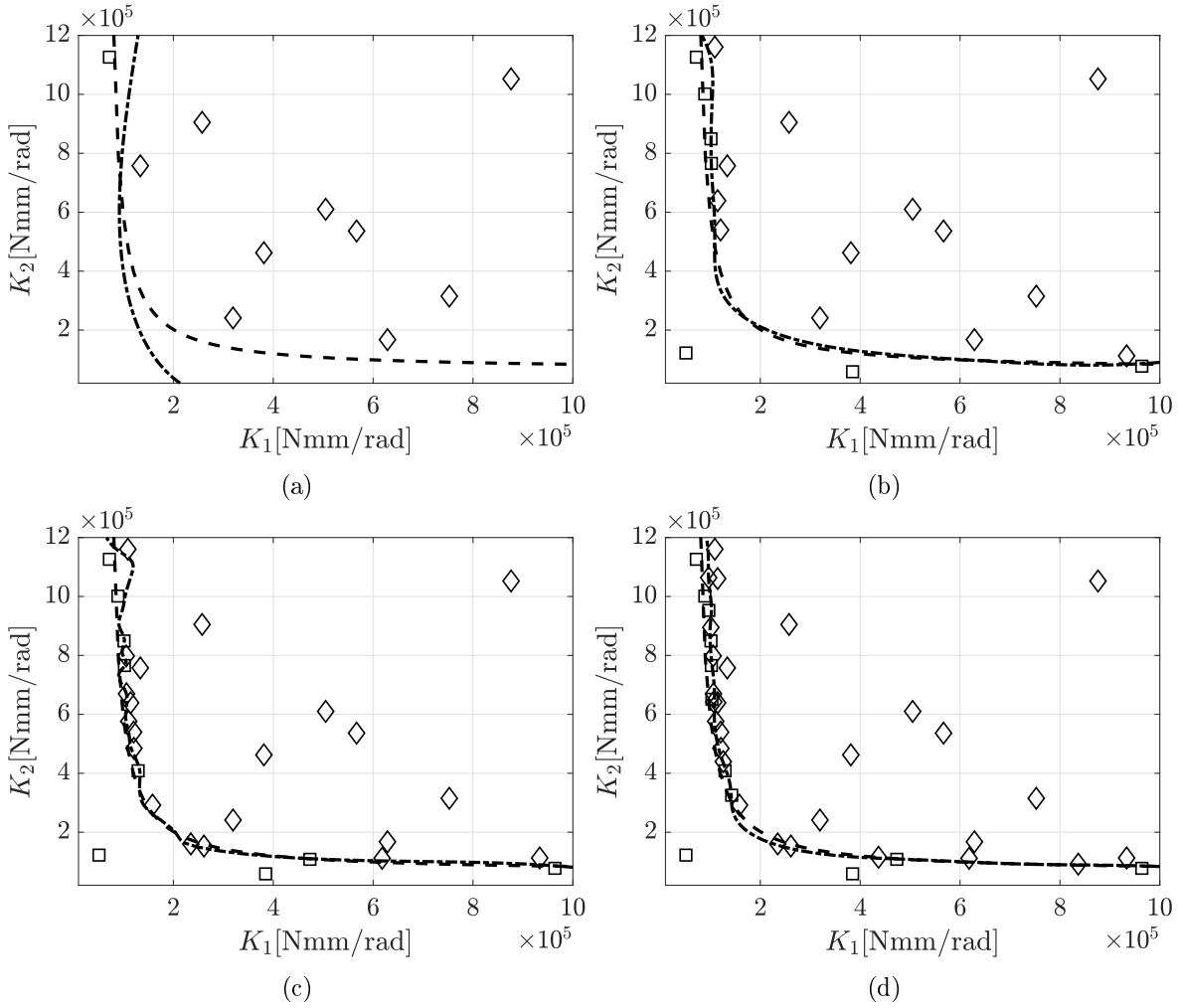

Figure 6: Results of the AK-HS procedure for (a) 10-sample ED (b) 20-sample ED (c) 30-sample ED and (d) 40-sample ED. Diamonds represent non-failed samples, squares represent failed samples, the dash line indicates the theoretical failure surface predicted by the Newmark equation and the dash-dot line indicates the failure surface predicted by the trained classifier.

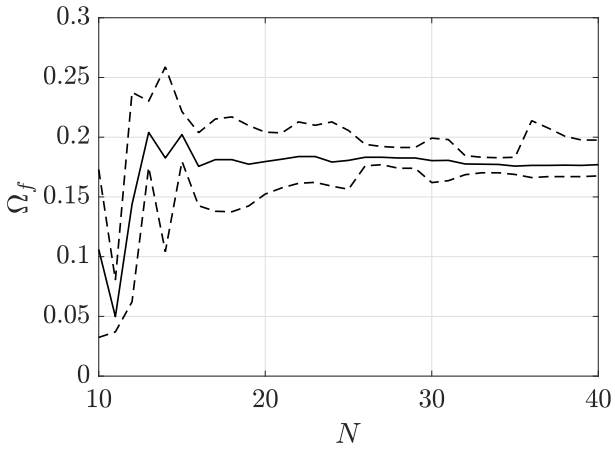

Figure 7: Convergence of the normalized failure domain area Ω_f and related 95 % confidence interval.

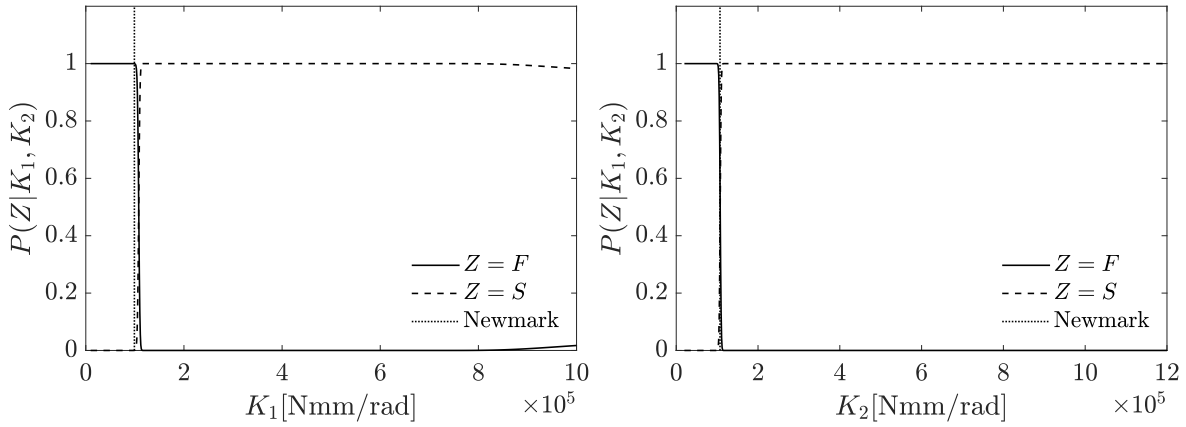

Figure 8: Safe/failure state classifier evaluated for two orthogonal sections of the support of the kriging meta-model: a) $K_2 = 600000$ Nmm/rad; b) $K_1 = 500000$ Nmm/rad.

adaptation of the active-learning kriging algorithm from the field of structural reliability. The effectiveness of the procedure is illustrated for a 3-degrees-of-freedom hybrid model consisting of an elastically restrained beam subjected to constant axial loading. Failure is associated with Euler buckling, which may occur or not depending on the rotational stiffness of the restraints for a given axial load. Experimental results demonstrated the effectiveness of the proposed procedure, which succeeded in training an accurate safe/failure state classifier with about 20 hybrid simulations. Out future work will address the extension of the proposed procedure to the case of PS with stochastic behavior.

6 Data availability statement

Some or all data, models, or code that support the findings of this study are available from the corresponding author upon reasonable request.

Acknowledgments

This work was supported by the Swiss Secretariat of Education Research and Innovation (SERI) - Swiss Space Office (SSO) [THERMICS Project (Thermo-Mechanical Virtualization of Hybrid Flax/Carbon Fiber Composite for Spacecraft Structures), MdP2016, grant number REF-1131-61001]. Also, the first author acknowledges Dr. Roland Schöbi for his comments and suggestions at the earliest onset of this research.

References

Abbiati, G., O. S. Bursi, P. Caperan, L. Di Sarno, F. J. Molina, F. Paolacci, and P. Pegon (2015). Hybrid simulation of a multi-span RC viaduct with plain bars and sliding bearings: Hybrid Simulations of a Multi-Span RC Viaduct. *Earthquake Engineering & Structural Dynamics 44*(13), 2221–2240.

Abbiati, G., P. Covi, N. Tondini, O. S. Bursi, and B. Stojadinović (2020). A Real-Time Hybrid Fire Simulation Method Based on Dynamic Relaxation and Partitioned Time Integration. *Journal of Engineering Mechanics 146*(9), 04020104.

Abbiati, G., V. Hey, and V. Rion (2018). Thermo-Mechanical Virtualization of Hybrid Flax/Carbon Fiber Composite for Spacecraft Structures (THERMICS). Technical report, ETH Zurich, Zurich, Switzerland.

Abbiati, G., V. La Salandra, O. S. Bursi, and L. Caracoglia (2018). A composite experimental dynamic substructuring method based on partitioned algorithms and localized Lagrange multipliers. *Mechanical Systems and Signal Processing 100*, 85–112.

Abbiati, G., I. Lanese, E. Cazzador, O. S. Bursi, and A. Pavese (2019). A computational framework for fast-time hybrid simulation based on partitioned time integration and state-space modeling. *Structural Control and Health Monitoring 26*(10).

Abbiati, G., R. Schöbi, B. Sudret, and B. Stojadinovic (2017). Structural reliability analysis using deterministic hybrid simulations and adaptive kriging metamodeling. In *Proceedings of the 16th World Conference on Earthquake Engineering (16WCEE)*.

Ahmadizadeh, M. and G. Mosqueda (2009). Online energy-based error indicator for the assessment of numerical and experimental errors in a hybrid simulation. *Engineering Structures 31*(9), 1987–1996.

Bažant, Z. P. and L. Cedolin (2010). *Stability of structures: elastic, inelastic, fracture and damage theories* (World Scientific ed ed.). Hackensack, NJ ; London: World Scientific Pub.

Bursi, O. S., G. Abbiati, E. Cazzador, P. Pegon, and F. J. Molina (2017). Nonlinear heterogeneous dynamic substructuring and partitioned FETI time integration for the development of low-discrepancy simulation models. *International Journal for Numerical Methods in Engineering 112*(9), 1253–1291.

Bursi, O. S., R. Ceravolo, S. Erlicher, and L. Zanotti Fragonara (2012). Identification of the hysteretic behaviour of a partial-strength steel-concrete moment-resisting frame structure subject to pseudodynamic tests. *Earthquake Engineering & Structural Dynamics 41*(14), 1883–1903.

Echard, B., N. Gayton, and M. Lemaire (2011). AK-MCS: An active learning reliability method combining Kriging and Monte Carlo Simulation. *Structural Safety 33*(2), 145–154.

Ligeikis, C. and R. Christenson (2020). Assessing structural reliability using real-time hybrid sub-structuring. *International Journal of Lifecycle Performance Engineering 4*(1-3), 158–183.

Marelli, S. and B. Sudret (2014). UQLab: A Framework for Uncertainty Quantification in Matlab. In *Vulnerability, Uncertainty, and Risk*, Liverpool, UK, pp. 2554–2563. American Society of Civil Engineers.

Mosqueda, G., B. Stojadinovic, J. Hanley, M. Sivaselvan, and A. M. Reinhorn (2008). Hybrid Seismic Response Simulation on a Geographically Distributed Bridge Model. *Journal of Structural Engineering 134*(4), 535–543.

Roy, C. J. and W. L. Oberkampf (2011). A comprehensive framework for verification, validation, and uncertainty quantification in scientific computing. *Computer Methods in Applied Mechanics and Engineering 200*(25-28), 2131–2144.

Santner, T., B. Williams, and W. Notz (2003). *The design and analysis of computer experiments*. New York, NY: Springer.

Sauder, T., S. Marelli, K. Larsen, and A. J. Sørensen (2018). Active truncation of slender marine structures: Influence of the control system on fidelity. *Applied Ocean Research 74*, 154–169.

Schöbi, R., B. Sudret, and S. Marelli (2017). Rare Event Estimation Using Polynomial-Chaos Kriging. *ASCE-ASME Journal of Risk and Uncertainty in Engineering Systems, Part A: Civil Engineering 3*(2).

Schellenberg, A. H., S. A. Mahin, and G. L. Fenves (2009). Advanced Implementation of Hybrid Simulation. Technical Report PERR 2009/104, Pacific Earthquake Engineering Research (PEER) Center, University of California, Berkeley.

Settles, B. (2009). Active Learning Literature Survey. Computer Sciences Technical Report 1648, University of Wisconsin–Madison.

Vapnik, V. (2013). *The nature of statistical learning theory*. Springer science & business media.

Vilsen, S., T. Sauder, A. Sørensen, and M. Føre (2019). Method for Real-Time Hybrid Model Testing of ocean structures: Case study on horizontal mooring systems. *Ocean Engineering 172*, 46–58.

Whyte, C. A., K. R. Mackie, and B. Stojadinovic (2016). Hybrid Simulation of Thermomechanical Structural Response. *Journal of Structural Engineering 142*(2), 04015107.

Worden, K., E. J. Cross, P. Gardner, R. J. Barthorpe, and D. J. Wagg (2020). On Digital Twins, Mirrors and Virtualisations. In R. Barthorpe (Ed.), *Model Validation and Uncertainty Quantification, Volume 3*, Cham, pp. 285–295. Springer International Publishing.

Yang, T. Y., B. Stojadinovic, and J. Moehle (2009). Hybrid simulation of a zipper-braced steel frame under earthquake excitation. *Earthquake Engineering & Structural Dynamics 38*(1), 95–113.